TECHNISCHE UNIVERSITÄT CHEMNITZ

Michael Weise

Simplified calculation of rHCT basis functions for an arbitrary splitting

CSC/15-01

Chemnitz Scientific Computing Preprints

Impressum:

Chemnitz Scientific Computing Preprints — ISSN 1864-0087
(1995–2005: Preprintreihe des Chemnitzer SFB393)

Herausgeber:
Professuren für
Numerische und Angewandte Mathematik
an der Fakultät für Mathematik
der Technischen Universität Chemnitz

Postanschrift:
TU Chemnitz, Fakultät für Mathematik
09107 Chemnitz
Sitz:
Reichenhainer Str. 41, 09126 Chemnitz

http://www.tu-chemnitz.de/mathematik/csc/

TECHNISCHE UNIVERSITÄT CHEMNITZ

Chemnitz Scientific Computing Preprints

Michael Weise

Simplified calculation of rHCT basis functions for an arbitrary splitting

CSC/15-01

Abstract

Reduced Hsieh–Clough–Tocher elements are triangular C^1-elements with only nine degrees of freedom. Simple formulas for the basis functions of reduced Hsieh–Clough–Tocher elements based on the edge vectors of the triangle have been given recently for a barycentric splitting. We generalise these formulas to the case of an arbitrary splitting point.

CSC/15-01 ISSN 1864-0087 January 2015

Contents

1 Introduction **1**

2 Basic definitions **1**

3 Mapping to the reference triangle **3**

4 Construction of the rHCT shape functions **4**

4.1 The basic functions 5
4.2 Ensuring Proposition 1 5
4.3 Ensuring Proposition 2 6
4.4 Ensuring Proposition 3 7
4.5 The final functions 11

Author's addresses:

Michael Weise
TU Chemnitz, Fakultät für Mathematik
09107 Chemnitz, Germany

http://www.tu-chemnitz.de/mathematik/

1 Introduction

Some relevant problems such as the biharmonic problem or the plate problem can be described by a partial differential equation of fourth order. The weak formulation of any such problem features functions from the Sobolev space H^2. Thus, the functions themselves as well as their first and second generalised derivatives have to be square-integrable over the considered domain. The natural approach to solving such problems numerically by the finite element method is to use conforming finite elements. This means that the FE basis functions belong to a finite-dimensional subspace of the appropriate space H^2. This is fulfilled for FE basis functions which are globally C^1-continuous.

One example of C^1-continuous elements is the reduced Hsieh–Clough–Tocher (rHCT) element, which goes back to [1]. It is a triangular element with piecewise cubic shape functions defined on three subtriangles. The shape functions are constructed in such a way that the resulting global basis functions are C^1-continuous. The element uses the values of the function and both first derivatives at all three vertices as degrees of freedom, which sums up to nine in total. Global C^1-continuity is achieved by inner C^1-continuity and the condition that the restriction of the normal derivative of any shape function to any element edge has to be linear with respect to the local line coordinate. The splitting into three subtriangles may be based on an arbitrary interior point, which is called splitting point.

There exist several approaches to the definition of rHCT shape functions. The method given in [2] constructs the final functions with the desired properties from basic master functions defined over the three subtriangles in several steps. The goal of the current article is to generalise the formulas of [2], which are given for a splitting based on the barycenter of the original triangle, to a splitting based on an arbitrary interior point. We closely follow the methods used in [2] while making the necessary changes. Formulas for an arbitrary splitting point have already been given in [3] based on barycentric coordinates and Bernstein–Bezier polynomials. The method presented here has the advantage of a relatively cheap implementation.

2 Basic definitions

Consider a split of the original triangle T with the vertices

$$a_j = [x_j, y_j]^\mathsf{T}, \quad j = 1, 2, 3$$

based on an arbitrary interior point

$$a_\mathrm{s} = [x_\mathrm{s}, y_\mathrm{s}]^\mathsf{T} \in \operatorname{int} T.$$

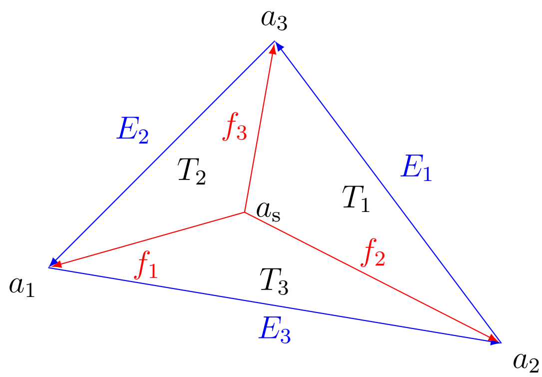

Figure 1: Triangle T with splitting

The three shape functions that belong to node a_j of the triangle T are written as a row vector

$$\mathit{\Psi}_j(a) = [\psi_j^{(0)}(a), \psi_j^{(1)}(a), \psi_j^{(2)}(a)]$$

and the full vector of all nine shape functions takes the form

$$\mathit{\Psi}(a) = [\mathit{\Psi}_1(a), \mathit{\Psi}_2(a), \mathit{\Psi}_3(a)]$$

at an arbitrary point $a = [x, y]^\mathsf{T}$. Shape functions with superscript (0) are related to the function value at the corresponding node and those with superscripts (1) and (2) are related to the function derivative with respect to x and y at the corresponding node.

In order to shorten the following expressions, we introduce some abbreviations to be used throughout the article. We use $x_{i,j}$ and $y_{i,j}$ to denote $x_i - x_j$ and $y_i - y_j$, respectively. This implies $x_{i,j} = -x_{j,i}$ and $y_{i,j} = -y_{j,i}$. Furthermore, all indices $k, k-1, k+1$ run from 1 to 3 and $k \pm 1$ is always understood implicitly as

$$k \pm 1 \;\mapsto\; \big((k \pm 1 - 1) \mod 3\big) + 1$$

to stay in the admissible index set $\{1, 2, 3\}$. Formulas that use k as an index are valid for $k = 1, 2, 3$.

The outer edges of the element are denoted by E_k and the inner edges by f_k. Their orientation is as given in Figure 1, which leads to the formulas

$$E_k = \begin{bmatrix} x_{k-1,k+1} \\ y_{k-1,k+1} \end{bmatrix} \text{ and } f_k = \begin{bmatrix} x_{k,\mathrm{s}} \\ y_{k,\mathrm{s}} \end{bmatrix}.$$

The subtriangle containing E_k is denoted T_k. We define normals of the outer and inner edges with the same length by

$$N_k = \underline{R}\, E_k, \quad n_k = \underline{R}\, f_k$$

with the rotation matrix

$$\underline{R} = \begin{bmatrix} 0 & -1 \\ 1 & 0 \end{bmatrix}.$$

3 Mapping to the reference triangle

Let each subtriangle T_k be mapped onto the reference triangle

$$\hat{T} = \{[\hat{x}, \hat{y}]^\mathsf{T} \in \mathbb{R}^2 : \hat{x} \geq 0, \hat{y} \geq 0, \hat{x} + \hat{y} \leq 1\}. \tag{1}$$

The subtriangle T_k has the edges E_k, f_{k+1}, and f_{k-1}, see Figure 1. Let the splitting point a_s be mapped to $\hat{a}_\mathrm{s} = [0, 0]^\mathsf{T}$, the edge f_{k+1} to the $\hat{x}$-axis and f_{k-1} to the $\hat{y}$-axis.

Then the mapping takes the form

$$a = \chi_{T_k}(\hat{a}) = \underline{J}_k\, \hat{a} + a_\mathrm{s}, \quad \hat{a} = \hat{\chi}_{T_k}(a) = \chi_{T_k}^{-1}(a) = \underline{J}_k^{-1}(a - a_\mathrm{s}) \quad \text{for } a \in T_k \tag{2}$$

with the Jacobians

$$\underline{J}_k = [f_{k+1} \vdots f_{k-1}] = \begin{bmatrix} x_{k+1,\mathrm{s}} & x_{k-1,\mathrm{s}} \\ y_{k+1,\mathrm{s}} & y_{k-1,\mathrm{s}} \end{bmatrix}.$$

Their determinants are abbreviated as

$$\mu_k = \det \underline{J}_k = x_{k+1,\mathrm{s}} y_{k-1,\mathrm{s}} - x_{k-1,\mathrm{s}} y_{k+1,\mathrm{s}}.$$

We now give two auxiliary relations that are used in the following sections. The transposed inverse of a Jacobian can be written as

$$\underline{J}_k^{-\mathsf{T}} = \frac{1}{\mu_k}[-n_{k-1} \vdots n_{k+1}]. \tag{3}$$

Furthermore, it holds

$$\begin{aligned} \mu_k y_{k,\mathrm{s}} + \mu_{k+1} y_{k+1,\mathrm{s}} + \mu_{k-1} y_{k-1,\mathrm{s}} = 0, \\ \mu_k x_{k,\mathrm{s}} + \mu_{k+1} x_{k+1,\mathrm{s}} + \mu_{k-1} x_{k-1,\mathrm{s}} = 0, \end{aligned} \tag{4}$$

which can be shown simply by expanding terms.

In the following section, the shape functions are formulated with the help of basic functions given on the reference triangle (1). Each of the three subtriangles is mapped to the reference triangle by an affine linear mapping (2) like illustrated in Figure 2.

4 Construction of the rHCT shape functions

The final shape functions are constructed to fulfil three propositions.

1. The functions Ψ are cubic polynomials in each subtriangle, are continuous within T, and fulfil

$$\Psi_j(a_i) = [1, 0, 0]\,\delta_{ij},$$
$$\nabla\Psi_j(a_i) = \begin{bmatrix} 0 & 1 & 0 \\ 0 & 0 & 1 \end{bmatrix} \delta_{ij} \quad \forall\, i, j = 1, 2, 3$$

   with the Kronecker delta

$$\delta_{ij} = \begin{cases} 1 & i = j, \\ 0 & i \neq j. \end{cases}$$

2. The normal derivatives of all functions are linear along outer element edges with respect to the local line coordinate.
3. The functions are C^1-continuous inside T.

The ∇ symbol denotes the gradient operator

$$\nabla = \left[\frac{\partial}{\partial x}, \frac{\partial}{\partial y}\right]^{\mathsf{T}}.$$

The final shape functions are defined with the help of basic functions and some transformations in order to assure the above propositions in the following subsections. The propositions guarantee the global C^1-continuity of the ansatz functions. In the following subsections, the same methods as in [2] are applied step by step to the more general setting here.

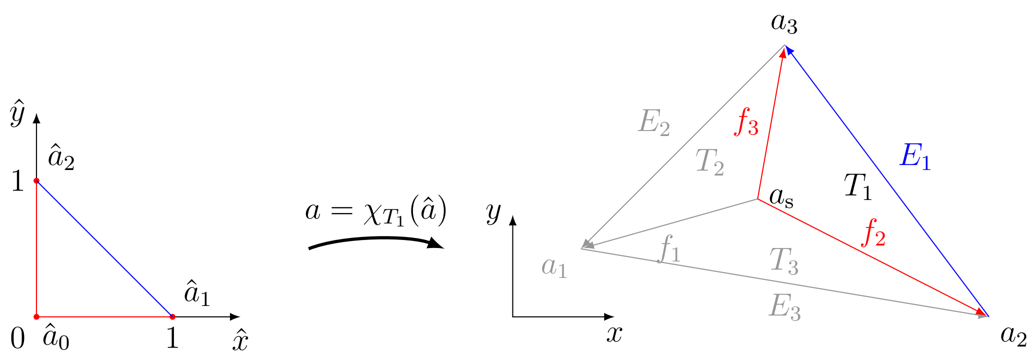

Figure 2: Mapping between the reference triangle and T_1

4.1 The basic functions

Denote the vertices of the reference triangle $\hat{T}$ by

$$\hat{a}_0 = \hat{a}_\mathrm{s} = \begin{bmatrix} 0 \\ 0 \end{bmatrix}, \quad \hat{a}_1 = \begin{bmatrix} 1 \\ 0 \end{bmatrix}, \quad \hat{a}_1 = \begin{bmatrix} 0 \\ 1 \end{bmatrix}.$$

The space of cubic polynomials over $\hat{T}$ can be spanned by the ten functions

$$\begin{aligned} \hat{\varPhi}_0(\hat{a}) &= (1 - \hat{x} - \hat{y})^2 \, [1 + 2\hat{x} + 2\hat{y},\ \hat{x},\ \hat{y}], \\ \hat{\varPhi}_1(\hat{a}) &= \hat{x}^2 \, [3 - 2\hat{x},\ \hat{x} - 1,\ \hat{y}], \\ \hat{\varPhi}_2(\hat{a}) &= \hat{y}^2 \, [3 - 2\hat{y},\ \hat{x},\ \hat{y} - 1], \\ \hat{\beta}(\hat{a}) &= \hat{x}\hat{y}(1 - \hat{x} - \hat{y}). \end{aligned} \tag{5}$$

They fulfil

$$\begin{aligned} \hat{\beta}(\hat{a}_i) &= 0 & \forall\, i = 0, 1, 2, \\ \hat{\varPhi}_j(\hat{a}_i) &= [1, 0, 0]\, \delta_{ij}, & \\ \hat{\nabla}\hat{\varPhi}_j(\hat{a}_i) &= \begin{bmatrix} 0 & 1 & 0 \\ 0 & 0 & 1 \end{bmatrix} \delta_{ij} & \forall\, i, j = 0, 1, 2 \end{aligned}$$

with the formal derivatives with respect to the reference coordinates

$$\hat{\nabla} = \left[\frac{\partial}{\partial \hat{x}}, \frac{\partial}{\partial \hat{y}} \right]^\mathsf{T}.$$

This property is similar to the desired Proposition 1, but uses $\hat{\nabla}$ instead of ∇. The function $\hat{\beta}$ is the cubic bubble function over $\hat{T}$.

4.2 Ensuring Proposition 1

We consider the basic functions $\hat{\varPhi}_1$ and $\hat{\varPhi}_2$ mapped to each subtriangle and scale them in order to fulfil Proposition 1. Let the 3×3 matrix

$$\underline{H}_k = \begin{bmatrix} 1 & 0 \quad 0 \\ 0 & \\ 0 & \underline{J}_k^\mathsf{T} \end{bmatrix}$$

for each $k = 1, 2, 3$. Define the initial basis $\varPhi_j^\mathrm{init}$, $j = 1, 2, 3$ within each subtriangle T_k by

$$\begin{aligned} \varPhi_{k+1}^\mathrm{init}|_{T_k}(\hat{x}) &= \hat{\varPhi}_1(\hat{x})\, \underline{H}_k, \\ \varPhi_{k-1}^\mathrm{init}|_{T_k}(\hat{x}) &= \hat{\varPhi}_2(\hat{x})\, \underline{H}_k; \end{aligned}$$

Φ_k^{init} vanishes on T_k. In summary, we have the 9 initial basis functions Φ_j^{init}, $j = 1, 2, 3$. The support of the three initial basis functions in Φ_j^{init} consists only of the two triangles T_{j+1} and T_{j-1}. One easily checks that Proposition 1 is fulfilled. For example, the gradient in T_k is transformed by

$$\nabla = \underline{J}_k^{-\mathsf{T}}\,\hat{\nabla}$$

and it holds

$$\begin{aligned}
\nabla\Phi_{k+1}^{\mathrm{init}}|_{T_k}(\hat{\chi}_{T_k}(a_{k+1})) &= \underline{J}_k^{-\mathsf{T}}\left(\hat{\nabla}\hat{\Phi}_1([1,0]^{\mathsf{T}})\right)\underline{H}_k \\
&= \underline{J}_k^{-\mathsf{T}}\begin{bmatrix}0 & 1 & 0\\ 0 & 0 & 1\end{bmatrix}\underline{H}_k \\
&= \begin{bmatrix}0 & 1 & 0\\ 0 & 0 & 1\end{bmatrix}
\end{aligned}$$

within T_k.

4.3 Ensuring Proposition 2

In each subtriangle, we add multiples of the bubble function $\hat{\beta}$ mapped to this subtriangle to fulfill Proposition 2. This does not interfere with Proposition 1 because the bubble function and its first derivatives are zero at all reference vertices.

With special chosen vectors $b_k^j \in \mathbb{R}^3$, let

$$\Phi_j|_{T_k}(\hat{x}) = \Phi_j^{\mathrm{init}}|_{T_k}(\hat{x}) + \hat{\beta}(\hat{x})\,(b_k^j)^{\mathsf{T}}$$

within T_k for $j = k+1$ and $j = k-1$. The vectors b_k^{k+1} and b_k^{k-1} are constructed such that the normal derivatives along outer edges E_k

$$\frac{\partial}{\partial N_k}\Phi_j|_{T_k} = \frac{\partial}{\partial N_k}\Phi_j^{\mathrm{init}}|_{T_k} + \frac{\partial}{\partial N_k}\hat{\beta}\,(b_k^j)^{\mathsf{T}}$$

are linear along the edge. The edge E_k is mapped to $[\hat{s}, 1-\hat{s}]^{\mathsf{T}} \in \hat{T}$, $s \in [0,1]$. This fact and the auxiliary equation

$$n_{k-1} - n_{k+1} = \underline{R}(f_{k-1} - f_{k+1}) = \underline{R}\,E_k = N_k$$

yield

$$\begin{aligned}
\frac{\partial}{\partial N_k}\hat{\beta}([\hat{s}, 1-\hat{s}]^\mathsf{T}) &= N_k^\mathsf{T} \underline{J}_k^{-\mathsf{T}} \Big(\hat{\nabla}\hat{\beta}([\hat{s}, 1-\hat{s}]^\mathsf{T})\Big) \\
&= N_k^\mathsf{T} \underline{J}_k^{-\mathsf{T}} \begin{bmatrix} -1 \\ -1 \end{bmatrix} \hat{s}(1-\hat{s}) \\
&= N_k^\mathsf{T} \tfrac{1}{\mu_k}(-n_{k+1} + n_{k-1})\, \hat{s}(1-\hat{s}) \\
&= \tfrac{1}{\mu_k} N_k^\mathsf{T} N_k\, \hat{s}(1-\hat{s}) \\
&= \tfrac{1}{\mu_k} |E_k|^2\, \hat{s}(1-\hat{s})
\end{aligned}$$

for the bubble function part and

$$\frac{\partial}{\partial N_k}\Phi_{k+1}^{\text{init}}|_{T_k}([\hat{s}, 1-\hat{s}]^\mathsf{T}) = N_k^\mathsf{T} \underline{J}_k^{-\mathsf{T}} \Big(\hat{\nabla}\hat{\Phi}_1([\hat{s}, 1-\hat{s}]^\mathsf{T})\Big)\underline{H}_k$$

for the initial basis function part in the case $j = k+1$. The matrix $\hat{\nabla}\hat{\Phi}_1$ can be calculated as

$$\hat{\nabla}\hat{\Phi}_1([\hat{s}, 1-\hat{s}]^\mathsf{T}) = \begin{bmatrix} 6 & -3 & 2 \\ 0 & 0 & -1 \end{bmatrix} \hat{s}(1-\hat{s}) + \begin{bmatrix} 0 & 1 & 0 \\ 0 & 0 & 1 \end{bmatrix} (1-\hat{s}).$$

Hence, the desired linear behaviour of Φ_{k+1} is obtained for

$$\begin{aligned}
(b_k^{k+1})^\mathsf{T} &= -\tfrac{\mu_k}{|E_k|^2} N_k^\mathsf{T} \underline{J}_k^{-\mathsf{T}} \begin{bmatrix} 6 & -3 & 2 \\ 0 & 0 & 1 \end{bmatrix} \underline{H}_k \\
&= [6E_k^\mathsf{T} f_{k-1} \vdots\, 3\mu_k n_k^\mathsf{T} + 2f_{k-1}^\mathsf{T}]/|E_k|^2.
\end{aligned}$$

For $j = k-1$, one analogously obtains

$$(b_k^{k-1})^\mathsf{T} = [-6E_k^\mathsf{T} f_{k+1} \vdots\, 3\mu_k n_k^\mathsf{T} + 2f_{k+1}^\mathsf{T}]/|E_k|^2.$$

Thus, Proposition 2 is fulfilled and the C^1-continuity between neighbouring elements is ensured.

4.4 Ensuring Proposition 3

It remains to ensure that the jumps of normal derivatives of the shape functions vanish along all inner edges f_i. Let the auxiliary functions Φ_0 be defined by

$$\Phi_0|_{T_k}(\hat{x}) = \hat{\Phi}_0(\hat{x})\underline{H}_k$$

on each subelement T_k. These functions vanish together with their gradients along all outer edges E_k. Therefore, adding linear combinations of Φ_0 does not interfere with Propositions 1 and 2. We use the ansatz

$$\Psi_j = \Phi_j + \Phi_0\, \underline{M}_j$$

with 3×3 matrices $\underline{M}_j$ and construct these such that all jumps of $\frac{\partial}{\partial n_i}\Psi_j$ vanish along f_i for all combinations of i and j.

In the following, the jumps of $\frac{\partial}{\partial n_i}\Phi_j$ and $\frac{\partial}{\partial n_i}\Phi_0$ are expressed as quadratic functions in the local line coordinate $\hat{s}$ representing edge f_i. They can be written as

$$\hat{s}(1-\hat{s})(t_i^{(j)})^\mathsf{T} \quad \text{and} \quad \hat{s}(1-\hat{s})s_j^\mathsf{T},$$

respectively, with vectors $t_i^{(j)}, s_j \in \mathbb{R}^3$. With the definition of the matrices $\underline{T}_j$ having the rows $(t_i^{(j)})^\mathsf{T}$ and $\underline{S}$ having the rows s_i^T, we get the desired matrices $\underline{M}_j$ as

$$\underline{M}_j = -\underline{S}^{-1}\underline{T}_j.$$

To calculate the jumps of $\frac{\partial}{\partial n_i}\Phi_j$, we start with $i = j+1$. The edge f_{j+1} separates the subtriangles T_j and T_{j-1}. In T_j the functions Φ_j vanish completely and it also holds

$$\nabla\Phi_j^{\text{init}}|_{T_{j-1}} = \begin{bmatrix} 0 & 0 & 0 \\ 0 & 0 & 0 \end{bmatrix}$$

along f_{j+1}. Thus, the jump in $\frac{\partial}{\partial n_{j+1}}\Phi_j$ stems from the bubble function in T_{j-1} only and reads

$$\left[\frac{\partial}{\partial n_{j+1}}\Phi_j\right]_{f_{j+1}} = -n_{j+1}^\mathsf{T}\underline{J}_{j-1}^{-\mathsf{T}}\left(\hat{\nabla}\hat{\beta}([0,\hat{s}]^\mathsf{T})\right)(b_{j-1}^j)^\mathsf{T}.$$

We have used the minus sign because f_{j+1} is mapped to the $\hat{y}$-axis of $\hat{T}$ in T_{j-1}; later we use the plus sign when an edge is mapped onto the $\hat{x}$-axis. From

$$\hat{\nabla}\hat{\beta}([0,\hat{s}]^\mathsf{T}) = \hat{s}(1-\hat{s})\begin{bmatrix} 1 \\ 0 \end{bmatrix}$$

and (3) we obtain

$$\begin{aligned}
(t_{j+1}^{(j)})^\mathsf{T} &= -n_{j+1}^\mathsf{T}\underline{J}_{j-1}^{-\mathsf{T}}\begin{bmatrix} 1 \\ 0 \end{bmatrix}(b_{j-1}^j)^\mathsf{T} \\
&= -n_{j+1}^\mathsf{T}\frac{1}{\mu_{j-1}}[-n_{j+1} \vdots n_j]\begin{bmatrix} 1 \\ 0 \end{bmatrix}(b_{j-1}^j)^\mathsf{T} \\
&= \frac{|f_{j+1}|^2}{\mu_{j-1}}(b_{j-1}^j)^\mathsf{T}.
\end{aligned}$$

For $i = j-1$, we analogously get

$$(t_{j-1}^{(j)})^\mathsf{T} = \frac{|f_{j-1}|^2}{\mu_{j+1}}(b_{j+1}^j)^\mathsf{T}.$$

from the same calculation within T_{j+1}.

The case $i = j$ leads to longer terms. The jump reads

$$\left[\frac{\partial}{\partial n_j}\Phi_j\right]_{f_j} = n_j^\mathsf{T}\Big(\underline{J}_{j-1}^{-\mathsf{T}}\big(\hat\nabla\hat\Phi_1([\hat s,0]^\mathsf{T})\big)H_{j-1} - \underline{J}_{j+1}^{-\mathsf{T}}\big(\hat\nabla\hat\Phi_2([0,\hat s]^\mathsf{T})\big)H_{j+1}\Big)$$
$$+ n_j^\mathsf{T}\Big(\underline{J}_{j-1}^{-\mathsf{T}}\big(\hat\nabla\hat\beta([\hat s,0]^\mathsf{T})\big)(b_{j-1}^j)^\mathsf{T} - \underline{J}_{j+1}^{-\mathsf{T}}\big(\hat\nabla\hat\beta([0,\hat s]^\mathsf{T})\big)(b_{j+1}^j)^\mathsf{T}\Big).$$

The difference of the bubble parts yields

$$\hat s(1-\hat s)\left(\frac{|f_j|^2}{\mu_{j-1}}b_{j-1}^j + \frac{|f_j|^2}{\mu_{j+1}}b_{j+1}^j\right)^\mathsf{T}$$

with analogous calculations like in the above cases. The remaining part consists of terms which are linear in $\hat s$ and vanish as well as factors of $\hat s(1-\hat s)$. These can be written as

$$\hat s(1-\hat s)\left(n_j^\mathsf{T}\frac{1}{\mu_{j-1}}[-n_{j+1} \vdots n_j]\begin{bmatrix}6 & -3 & 0\\ 0 & 0 & -1\end{bmatrix}\begin{bmatrix}1 & 0 & 0\\ 0 & f_j^\mathsf{T} & \\ 0 & f_{j+1}^\mathsf{T} & \end{bmatrix}\right.$$
$$\left.-n_j^\mathsf{T}\frac{1}{\mu_{j+1}}[-n_j \vdots n_{j-1}]\begin{bmatrix}0 & -1 & 0\\ 6 & 0 & -3\end{bmatrix}\begin{bmatrix}1 & 0 & 0\\ 0 & f_{j-1}^\mathsf{T} & \\ 0 & f_j^\mathsf{T} & \end{bmatrix}\right)$$
$$= \hat s(1-\hat s)\Big(\tfrac{1}{\mu_{j-1}}\big[-6n_j^\mathsf{T}n_{j+1} \vdots 3n_j^\mathsf{T}n_{j+1}f_j^\mathsf{T} - |f_j|^2 f_{j+1}\big]$$
$$+ \tfrac{1}{\mu_{j+1}}\big[-6n_j^\mathsf{T}n_{j-1} \vdots 3n_j^\mathsf{T}n_{j-1}f_j^\mathsf{T} - |f_j|^2 f_{j-1}\big]\Big).$$

From (4) follows

$$\frac{1}{\mu_{j-1}}n_{j+1} + \frac{1}{\mu_{j+1}}n_{j-1} = -\frac{\mu_j}{\mu_{j-1}\mu_{j+1}}n_j, \qquad \frac{1}{\mu_{j-1}}f_{j+1} + \frac{1}{\mu_{j+1}}f_{j-1} = -\frac{\mu_j}{\mu_{j-1}\mu_{j+1}}f_j$$

and the above formula simplifies to

$$\hat s(1-\hat s)\frac{\mu_j}{\mu_{j-1}\mu_{j+1}}|f_j|^2[6 \vdots -3f_j^\mathsf{T} + f_j^\mathsf{T}] = \hat s(1-\hat s)\frac{\mu_j}{\mu_{j-1}\mu_{j+1}}|f_j|^2\,(c^j)^\mathsf{T}$$

with the abbreviation $c^j := [6 \vdots -2f_j^\mathsf{T}]^\mathsf{T}$. All parts together lead to

$$t_j^{(j)} = \frac{|f_j|^2}{\mu_{j-1}}b_{j-1}^j + \frac{|f_j|^2}{\mu_{j+1}}b_{j+1}^j + \frac{|f_j|^2\mu_j}{\mu_{j+1}\mu_{j-1}}c_j.$$

It remains to calculate the rows of $\underline{S}$ by evaluating the jumps of $\frac{\partial}{\partial n_j}\Phi_0$ at f_j,

$$\left[\frac{\partial}{\partial n_j}\Phi_0\right]_{f_j} = n_j^\mathsf{T}\Big(\underline{J}_{j-1}^{-\mathsf{T}}\big(\hat\nabla\hat\Phi_0([\hat s,0]^\mathsf{T})\big)H_{j-1} - \underline{J}_{j+1}^{-\mathsf{T}}\big(\hat\nabla\hat\Phi_0([0,\hat s]^\mathsf{T})\big)H_{j+1}\Big).$$

Again we encounter a linear part which vanishes and factors of $\hat{s}(1-\hat{s})$, which can be written as

$$\hat{s}(1-\hat{s})\left(n_j^\mathsf{T}\frac{1}{\mu_{j-1}}[-n_{j+1} \vdots n_j]\begin{bmatrix}-6 & -3 & 0\\ -6 & -2 & -1\end{bmatrix}\begin{bmatrix}1 & 0 & 0\\ 0 & f_j^\mathsf{T} & \\ 0 & f_{j+1}^\mathsf{T} & \end{bmatrix}\right.$$
$$\left.-n_j^\mathsf{T}\frac{1}{\mu_{j+1}}[-n_j \vdots n_{j-1}]\begin{bmatrix}-6 & -1 & -2\\ -6 & 0 & -3\end{bmatrix}\begin{bmatrix}1 & 0 & 0\\ 0 & f_{j-1}^\mathsf{T} & \\ 0 & f_j^\mathsf{T} & \end{bmatrix}\right)$$
$$= \hat{s}(1-\hat{s})\Big(\tfrac{1}{\mu_{j-1}}\Big[6n_j^\mathsf{T}n_{j+1} - 6|f_j|^2 \vdots (3n_j^\mathsf{T}n_{j+1} - 2|f_j|^2)f_j^\mathsf{T} - |f_j|^2 f_{j+1}^\mathsf{T}\Big]$$
$$+ \tfrac{1}{\mu_{j+1}}\Big[6n_j^\mathsf{T}n_{j-1} - 6|f_j|^2 \vdots (3n_j^\mathsf{T}n_{j-1} - 2|f_j|^2)f_j^\mathsf{T} - |f_j|^2 f_{j-1}^\mathsf{T}\Big]\Big).$$

Analogous transformations like above and the abbreviation $\mu_+ := \mu_1 + \mu_2 + \mu_3$ yield

$$\ldots = \hat{s}(1-\hat{s})\begin{bmatrix} -6\frac{\mu_j}{\mu_{j-1}\mu_{j+1}}|f_j|^2 - 6(\frac{1}{\mu_{j-1}} + \frac{1}{\mu_{j+1}})|f_j|^2 \\ (-3\frac{\mu_j}{\mu_{j-1}\mu_{j+1}}|f_j|^2 - 2(\frac{1}{\mu_{j-1}} + \frac{1}{\mu_{j+1}})|f_j|^2 + \frac{\mu_j}{\mu_{j-1}\mu_{j+1}}|f_j|^2)f_j\end{bmatrix}$$
$$= \hat{s}(1-\hat{s})|f_j|^2\tfrac{\mu_+}{\mu_{j-1}\mu_{j+1}}[-6 \vdots -2f_j^\mathsf{T}].$$

Therefore,

$$s_j^\mathsf{T} = |f_j|^2\tfrac{\mu_+}{\mu_{j-1}\mu_{j+1}}[-6 \vdots -2f_j^\mathsf{T}].$$

Note that a multiplication of all i-th rows of $\underline{T}_j$ and $\underline{S}$ with the same factor cancels out in the system

$$\underline{M}_j = -\underline{S}^{-1}\underline{T}_j.$$

Thus, we may renew the definition of the rows of $\underline{T}_j$ and $\underline{S}$ by dividing all i-th rows by $\frac{|f_i|^2}{\mu_{i-1}\mu_{i+1}}$ which yields the simplified matrices

$$\underline{S} = -2\mu_+\begin{bmatrix}3 & f_1^\mathsf{T}\\ 3 & f_2^\mathsf{T}\\ 3 & f_3^\mathsf{T}\end{bmatrix}$$

and

$$\underline{T}_k = e_{k-1}(\mu_k b_{k+1}^k)^\mathsf{T} + e_{k+1}(\mu_k b_{k-1}^k)^\mathsf{T} + e_k(\mu_{k-1}b_{k+1}^k + \mu_{k+1}b_{k-1}^k + \mu_k c^k)^\mathsf{T}.$$

The e_j in the formula for $\underline{T}_k$ denote the j-th unit vectors with $(e_j)_i = \delta_{ij}$.

4.5 The final functions

The formulas for all shape functions on subtriangle T_k read

$$\begin{aligned}
\Psi_k|_{T_k} &= \hat{\Phi}_0\, \underline{H}_k\, \underline{M}_k, \\
\Psi_{k+1}|_{T_k} &= \hat{\Phi}_1\, \underline{H}_k + \hat{\beta}\,(b_k^{k+1})^\mathsf{T} + \hat{\Phi}_0\, \underline{H}_k\, \underline{M}_{k+1}, \\
\Psi_{k-1}|_{T_k} &= \hat{\Phi}_2\, \underline{H}_k + \hat{\beta}\,(b_k^{k-1})^\mathsf{T} + \hat{\Phi}_0\, \underline{H}_k\, \underline{M}_{k-1}
\end{aligned} \tag{6}$$

with the basic functions

$$\begin{aligned}
\hat{\Phi}_0(\hat{a}) &= (1-\hat{x}-\hat{y})^2\,[1+2\hat{x}+2\hat{y},\ \hat{x},\ \hat{y}], \\
\hat{\Phi}_1(\hat{a}) &= \hat{x}^2\,[3-2\hat{x},\ \hat{x}-1,\ \hat{y}], \\
\hat{\Phi}_2(\hat{a}) &= \hat{y}^2\,[3-2\hat{y},\ \hat{x},\ \hat{y}-1], \\
\hat{\beta}(\hat{a}) &= \hat{x}\hat{y}(1-\hat{x}-\hat{y})
\end{aligned}$$

given on the reference triangle

$$\hat{T} = \{[\hat{x},\hat{y}]^\mathsf{T} \in \mathbb{R}^2 : \hat{x} \geq 0, \hat{y} \geq 0, \hat{x}+\hat{y} \leq 1\}$$

and the auxiliary terms

$$\begin{aligned}
\underline{H}_k &= \begin{bmatrix} 1 & 0 \quad 0 \\ 0 & \\ 0 & \underline{J}_k^\mathsf{T} \end{bmatrix} = \begin{bmatrix} 1 & 0 & 0 \\ 0 & x_{k+1,\mathrm{s}} & y_{k+1,\mathrm{s}} \\ 0 & x_{k-1,\mathrm{s}} & y_{k-1,\mathrm{s}} \end{bmatrix} = \begin{bmatrix} 1 & 0 \quad 0 \\ 0 & f_{k+1}^\mathsf{T} \\ 0 & f_{k-1}^\mathsf{T} \end{bmatrix}, \\
b_k^{k+1} &= \frac{1}{|E_k|^2} \begin{bmatrix} 6E_k^\mathsf{T} f_{k-1} \\ 3\mu_k N_k + 2|E_k|^2 f_{k-1} \end{bmatrix}, \\
b_k^{k-1} &= \frac{1}{|E_k|^2} \begin{bmatrix} -6E_k^\mathsf{T} f_{k+1} \\ 3\mu_k N_k + 2|E_k|^2 f_{k+1} \end{bmatrix}, \\
c^k &= \begin{bmatrix} 6 \\ -2f_k \end{bmatrix}, \\
\underline{S} &= -2\mu_+ \begin{bmatrix} 3 & f_1^\mathsf{T} \\ 3 & f_2^\mathsf{T} \\ 3 & f_3^\mathsf{T} \end{bmatrix} = -2\mu_+ \begin{bmatrix} 3 & x_{1,\mathrm{s}} & y_{1,\mathrm{s}} \\ 3 & x_{2,\mathrm{s}} & y_{2,\mathrm{s}} \\ 3 & x_{3,\mathrm{s}} & y_{3,\mathrm{s}} \end{bmatrix}, \\
\underline{S}^{-1} &= -\frac{1}{6\mu_+^2} \begin{bmatrix} \mu_1 & \mu_2 & \mu_3 \\ 3N_1 & 3N_2 & 3N_3 \end{bmatrix}, \\
\underline{T}_k &= e_{k-1}(\mu_k b_{k+1}^k)^\mathsf{T} + e_{k+1}(\mu_k b_{k-1}^k)^\mathsf{T} + e_k(\mu_{k-1} b_{k+1}^k + \mu_{k+1} b_{k-1}^k + \mu_k c^k)^\mathsf{T}, \\
\underline{M}_k &= -\underline{S}^{-1}\underline{T}_k.
\end{aligned}$$

In a finite element implementation, the ansatz functions are mainly needed for the setup of the element stiffness matrix, which is usually done by Gaussian integration. The integration routine runs over all Gaussian points on the reference triangle separately for all three subtriangles. The desired function and derivative values at each Gaussian point are obtained with the above formula (6). All auxiliary terms are constant over the element. Therefore, they have to be calculated only once for each element during the setup of the element stiffness matrix. This leads to a relatively cheap implementation.

References

[1] R. W. Clough and J. L. Tocher. Finite element stiffness matrices for analysis of plates in bending. In *Proceedings of the Conference on Matrix Methods in Structural Mechanics*, pages 515–545, 1965.

[2] A. Meyer. A simplified calculation of reduced HCT-basis functions in a finite element context. *Computational Methods in Applied Mathematics*, 12(4):486–499, 2012.

[3] A. S. Peker, J. E. Lavery, and S.-C. Fang. A reduced hsieh–clough–tocher element with splitting based on an arbitrary interior point. *Journal of Mathematical Analysis and Applications*, 333(1):500 – 504, 2007. Special issue dedicated to William Ames.

Some titles in this CSC and the former SFB393 preprint series:

09-01 R. Unger. Obstacle Description with Radial Basis Functions for Contact Problems in Elasticity. January 2009.

09-02 U.-J. Görke, S. Kaiser, A. Bucher, R. Kreißig. A fast and efficient algorithm to compute BPX- and overlapping preconditioner for adaptive 3D-FEM. February 2009.

09-03 J. Glänzel. Kurzvorstellung der 3D-FEM Software SPC-PM3AdH-XX. January 2009.

09-04 P. Benner, Th. Mach. On the QR Decomposition of H-Matrices. July 2009.

09-05 M. Meyer. Parameter identification problems for elastic large deformations - Part I: Model and solution of the inverse problem. October 2009.

09-06 M. Meyer. Parameter identification problems for elastic large deformations - Part II: Numerical solution and results. November 2009.

09-07 P. Benner, S. Hein. Model predictive control based on an LQG design for time-varying linearizations. November 2009.

09-08 U. Baur, C. A. Beattie, P. Benner, S. Gugercin. Interpolatory Projection Methods for Parameterized Model Reduction. November 2009.

09-09 J. Saak, S. Schlömer. RRQR-MEX - Linux and Windows 32bit Matlab Mex-Files for the rank revealing QR factorization. December 2009.

09-10 M. Köhler, J. Saak. Efficiency improving implementation techniques for large scale matrix equation solvers. December 2009.

09-11 P. Benner, H. Faßbender. On the numerical solution of large-scale sparse discrete-time Riccati equations. December 2009.

10-01 A. Meyer, P. Steinhorst. Modellierung und Numerik wachsender Risse bei piezoelektrischem Material. May 2010.

10-02 M. Balg, A. Meyer. Numerische Simulation nahezu inkompressibler Materialien unter Verwendung von adaptiver, gemischter FEM. June 2010.

10-03 M. Weise, A. Meyer. Grundgleichungen für transversal isotropes Materialverhalten. July 2010.

10-04 M. K. Bernauer, R. Herzog. Optimal Control of the Classical Two-Phase Stefan Problem in Level Set Formulation. October 2010.

11-01 P. Benner, M.-S. Hossain, T. Stykel. Low-rank iterative methods of periodic projected Lyapunov equations and their application in model reduction of periodic descriptor systems. February 2011.

11-02 G. Of, G. J. Rodin, O. Steinbach, M. Taus. Coupling Methods for Interior Penalty Discontinuous Galerkin Finite Element Methods and Boundary Element Methods. September 2011.

12-01 J. Rückert, A. Meyer. Kirchhoff Plates and Large Deformation. April 2012.

12-02 A. Meyer. The Koiter shell equation in a coordinate free description. February 2012.

12-03 M. Balg, A. Meyer. Fast simulation of (nearly) incompressible nonlinear elastic material at large strain via adaptive mixed FEM. July 2012.

13-01 A. Meyer. The Koiter shell equation in a coordinate free description – extended. September 2013.

13-02 R. Schneider. With a new refinement paradigm towards anisotropic adaptive FEM on triangular meshes. September 2013.

13-03 A. Meyer. The linear Naghdi shell equation in a coordinate free description. November 2013.

14-01 A. Meyer. Programmbeschreibung SPC-PM3-AdH-XX - Teil 1. March 2014.

14-02 A. Meyer. Programmbeschreibung SPC-PM3-AdH-XX - Teil 2. April 2014.

14-03 J. Glänzel, R. Unger. High Quality FEM-Postprocessing and Visualization Using a Gnuplot Based Toolchain. July 2014.

14-04 M. Weise. A note on the second derivatives of rHCT basis functions. October 2014.

The complete list of CSC and SFB393 preprints is available via
`http://www.tu-chemnitz.de/mathematik/csc/`

Chemnitz Scientific Computing Preprints – ISSN 1864-0087